

Voltage Control of Droplet Interface Bilayer Lipid Membrane Dimensions

Srikoundinya Punnamaraju and Andrew J. Steckl*

Nanoelectronics Laboratory, University of Cincinnati, Cincinnati, Ohio 45221-0030, United States

Received May 7, 2010. Revised Manuscript Received November 8, 2010

A novel approach to control the area of *anchor-free* droplet interface bilayer (DIB) lipid membranes is presented. Unsupported DIB lipid membranes are formed at the interface of phospholipid-coated aqueous droplets dispensed in dodecane oil. Using electrodes inserted into the droplets, an external voltage is applied which modulates the effective DIB area. Electrical (capacitance or current) and optical (imaging of DIB lateral length) recordings were simultaneously performed. Alpha-hemolysin (α HL) single channel insertions into the DIB were recorded. Currents across the DIB were measured as a function of voltage and α HL concentration in the droplets. Nonlinear response is observed for current, DIB lateral length and area, and capacitance with respect to voltage. Voltage induced changes in interfacial tension modulated the DIB–oil contact angle and the membrane contact length, which provided control of membrane dimensions. Comparison of these results is made to the electrowetting effect, which is also governed by effect of voltage on the interfacial tension. This approach provides *active* control of the number of ion channels inserted into the DIB.

I. Introduction

The protective wall around biological cells is primarily composed of a lipid bilayer membrane. This selectively permeable barrier separates the intracellular components from the extracellular environment and is the site of numerous vital biological functions.¹ In particular, certain transmembrane proteins act as ion channels, selectively controlling the transport of specific ions across the membrane. This is a fundamental regulation process of many physiological functions.

The investigation of natural cell membranes involves many difficulties, both in sample preparation and measurement techniques. Synthetic lipid bilayers dating back to the 1960s^{2,3} are simplified equivalents of biological membranes that are utilized in understanding membrane proteins and performing drug screening. Artificial lipid bilayers fall primarily into two broad categories: supported and unsupported. Supported membranes are formed on a substrate and are relatively easy to produce. However, the substrate restricts the natural shape and movement of the membrane and limits access to only one side of the membrane. Edge-supported membranes are formed on an aperture in a solid wall separating two fluid compartments. These membranes are planar, and maximum membrane area is predefined by the size of the aperture. Finally, true unsupported membranes (such as those formed in vesicles) can have more cell-like curved shapes, and their dimensions can be changed by various techniques.

To form an unsupported droplet interface bilayer (DIB) membrane, aqueous droplets are first dispensed in lipid oil, producing a lipid *monolayer* self-assembled around each droplet.^{4,5} This approach stems from early contributions made by Tsofina et al.⁶ The first published DIB report⁷ was from the group of Takeuchi

at the University of Tokyo who formed lipid *bilayers* by bringing monolayer coated droplets into contact. The collaboration of Bayley, Holden, Needham, and Wallace groups based mainly at Oxford has produced^{8–13} many important advances in DIB functionality and applications. An approach similar to DIB was demonstrated¹⁴ by the Schmidt group at UCLA using progressive injection of water on both sides of a microfluidic channel filled with lipid oil to form lipid bilayer membrane. Electrofluidic approaches to the automation of the DIB formation process have been reported by the group of Morgan¹⁵ at Southampton and the Schmidt–Kim groups at UCLA.¹⁶ Morgan's group also demonstrated¹⁷ lipid bilayer formation from falling droplets. The Leo group at Virginia Tech applied external feedback control to accurately measure¹⁸ currents across DIBs. They have also demonstrated the versatility of DIBs in forming biomolecular networks^{19–21} and controlled DIB overlap using deformable flexible substrates.²² Aguilera and Alcaraz reported²³ simple DIB electrical circuits as an augment to the work by the Oxford group.¹³ The Lavan group at Yale University and NIST used DIB

(8) Holden, M. A.; Needham, D.; Bayley, H. *J. Am. Chem. Soc.* **2007**, *129*, 8650–8655.

(9) Hwang, W. L.; Holden, M. A.; White, S.; Bayley, H. *J. Am. Chem. Soc.* **2007**, *129*, 11854–11864.

(10) Hwang, W. L.; Chen, M.; Cronin, B.; Holden, M. A.; Bayley, H. *J. Am. Chem. Soc.* **2008**, *130*, 5878–5879.

(11) Syeda, R.; Holden, M. A.; Hwang, W. L.; Bayley, H. *J. Am. Chem. Soc.* **2008**, *130*, 15543–15548.

(12) Bayley, H.; Cronin, B.; Heron, A.; Holden, M. A.; Hwang, W. L.; Syeda, R.; Thompson, J. R.; Wallace, M. I. *Mol. Biosyst.* **2008**, *4*, 1191–1208.

(13) Maglia, G.; Heron, A. J.; Hwang, W. L.; Holden, M. A.; Mikhailova, E.; Li, Q.; Cheley, S.; Bayley, H. *Nature Nanotechnol.* **2009**, *4*, 437–440.

(14) Malmstadt, N.; Nash, M. A.; Purnell, R. F.; Schmidt, J. J. *Nano Lett.* **2006**, *6*, 1961–1965.

(15) Aghdaei, S.; Sandison, M. E.; Zagnoni, M.; Green, N. G.; Morgan, H. *Lab Chip* **2008**, *8*, 1617–1620.

(16) Poulos, J. L.; Nelson, W. C.; Jeon, T.-J.; Kim, C.-J.; Schmidt, J. J. *Appl. Phys. Lett.* **2009**, *95*, 013706–1–013706-3.

(17) Zagnoni, M.; Sandison, M. E.; Marius, P.; Morgan, H. *Anal. Bioanal. Chem.* **2009**, *393*, 1601–1605.

(18) Sarles, S. A.; Leo, D. J. *J. Intell. Mater. Syst. Struct.* **2009**, *20*, 1233–1247.

(19) Sarles, S. A.; Bavarsad, P. G.; Leo, D. J. *Proc. SPIE* **2009**, *7288*, 72880H–1–72880H-10.

(20) Sarles, S. A.; Leo, D. J. *Lab Chip* **2010**, *10*, 710–717.

(21) Creasy, M. A.; Leo, D. J. *Smart Mater. Struct.* **2010**, *19*, 1–7.

(22) Sarles, S. A.; Leo, D. J. *Anal. Chem.* **2010**, *82*, 959–966.

(23) Aguilera, V. M.; Alcaraz, A. *Nat. Nanotechnol.* **2009**, *4*, 403–404.

*To whom correspondence should be addressed. E-mail: a.steckl@uc.edu.

(1) Ottova, A.; Tien, H. T. *The Lipid Bilayer Principle: A Historic Perspective and Some Highlights*; Chapter 1, Advances in Planar Lipid Bilayers and Liposomes; Elsevier Academic Press: San Diego, California, 2005; Vol. 1.

(2) Tien, H. T.; Ottova, A. L. *J. Membr. Sci.* **2001**, *189*, 83–117.

(3) Edidin, M. *Nat. Rev. Mol. Cell Biol.* **2003**, *4*, 414–418.

(4) Hase, M.; Yamada, A.; Hamada, T.; Yoshikawa, K. *Chem. Phys. Lett.* **2006**, *426*, 441–444.

(5) Thompson, J. R.; Heron, A. J.; Santoso, Y.; Wallace, M. I. *Nano Lett.* **2007**, *7*, 3875–3878.

(6) Tsofina, L. M.; Liberman, E. A.; Babakov, A. V. *Nature* **1966**, *212*, 681–683.

(7) Funakoshi, K.; Suzuki, H.; Takeuchi, S. *Anal. Chem.* **2006**, *78*, 8169–8174.

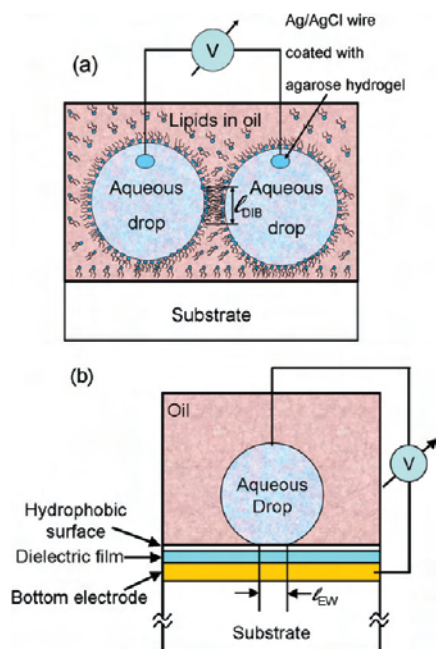


Figure 1. Schematic diagrams: (a) droplet interface bilayer (DIB) showing lipid monolayer coated aqueous droplets held by Ag/AgCl electrodes; (b) electro-wetting on dielectric structure.

as a biological battery.²⁴ Stanley et al. at Imperial College London reported a microfluidic approach for high-throughput DIB formation.²⁵ Finally, Dixit and colleagues at SRI International have reported²⁶ the light-driven formation of DIBs. Bayley and Wallace groups at Oxford also reported droplet hydrogel bilayers (DHBs)^{5,27,28} which are similar to DIBs except that there is only one lipid monolayer coated droplet instead of two.

This paper presents a novel approach to control the properties of unsupported lipid bilayers in DIBs using an externally applied electric field. This method produced reversible and reproducible control of the DIB dimensions. The DIB structure is shown schematically in Figure 1a. The diagram indicates the formation of a DIB between two lipid coated aqueous droplets in contact in a lipid oil environment. The diagram also shows Ag/AgCl wire electrodes inserted into the droplets for applying the voltage. Both DC and AC voltage were able to control the lateral extent (l_{DIB}) of the lipid bilayer membrane.

It is instructive to compare the case of the two aqueous droplets forming the DIB in lipid oil ambient to the case of an aqueous droplet placed on a hydrophobic surface in oil ambient (Figure 1b). In both cases, applying an external voltage modifies the dimensions of the droplet region in contact with either the second droplet (l_{DIB}) or in contact with the fluoropolymer (l_{EW}). In the latter case, the electric field provides an electro-wetting (EW) force countering the effect of the surface tension mismatch between water, oil, and the fluoropolymer.^{29,30} This causes the droplet to decrease its contact angle (CA) and increase its contact length, in other words to wet the surface. As will be shown later in

this paper, the voltage control of the DIB appears to be due to the voltage induced changes in interfacial surface tension, an effect that is similar to the EW effect. Earlier reported work on membrane area changes with voltage were primarily based on aperture based lipid bilayers.^{31–38} Babakov et al.³¹ first reported that changes in voltage affect membrane capacitance and area by acting against surface tension. White et al.³⁵ reported very small changes in membrane area and capacitance linearly proportional to the square of the applied voltage. Requena et al.³⁶ reported a modified version of Lippmann equation for contact angle changes at the Plateau–Gibbs border. However, reported changes in contact angles with voltage were based on calculations, not direct measurements. White et al.³⁸ reported changes in membrane area with applied voltage for planar bilayers. Membrane area change (experimental) was reported to be only about 10% for a voltage change from 0 to 100 mV. This limitation could be due to the fact that edges of the membrane are anchored by the aperture. As can be seen from their results, the percentage change in lipid bilayer area has a linear dependence on square of voltage, which is also seen in the DIB results presented here. Interestingly, changes are relatively more significant in case of DIB.

II. Experimental Procedure

A. Lipid Oil. Phospholipid molecules consist of a hydrophilic polar headgroup and two hydrophobic fatty acid tails. DOPC (1,2-dioleoyl-*sn*-glycero-3-phosphocholine lyophilized powder, Sigma-Aldrich) and DPhPC (1,2-diphytanoyl-*sn*-glycero-3-phosphocholine, Avanti Polar Lipids) were utilized as the main phospholipids. DOPC is unsaturated, and DPhPC is saturated. For fluorescence imaging of lipid-monolayer coating around each aqueous droplet, *N*-(fluorescein-5-thiocarbonyl)-1,2-dihexadecanoyl-*sn*-glycero-3-phosphoethanolamine, triethylammonium salt (fluorescein DHPE, Invitrogen) phospholipid was used in minute quantities along with DOPC. Fluorescein DHPE excitation and emission spectral maxima in methanol are 496 and 519 nm, respectively. The net charge on the selected phospholipids is zero at pH = 7. Dodecane oil (31 g, Acros Organics) was mixed with DOPC (24.79 mg) and F362 DHPE (1.1 mg) phospholipids and then sonicated for 50 min in warm water to obtain approximately 20 μ M F362 DHPE and 1 mM DOPC lipid oil. In another experiment set, DOPC concentration was set at 8 mg/mL of dodecane. For experiments with DPhPC lipid oil, the DPhPC concentration was set at 5 mg/mL in dodecane.

B. Droplets. Several volumes and types of aqueous droplets were used in DIB experiments. The droplet volume used in electrical experiments varied from a few nanoliters to 500 nL. For various results reported in this paper that involved voltage application, 1 \times phosphate buffered saline (PBS, pH 7.4, Invitrogen), “150 mM KCl-10 mM HEPES” (pH 7.4), and ASTM Type1 DI H₂O (Ricca Chemical Company) droplets were mainly used. For ion current measurements, alpha-hemolysin (α HL) from Sigma-Aldrich was mixed in “KCl-HEPES” solution and both droplets of DIB had the same concentration of alpha-hemolysin.

C. Substrates. Rectangular microchannels were fabricated on acrylic sheets using laser cutting. After laser cut, acrylic samples with rectangular channels were bonded to a bottom plastic slide using 5 min epoxy. These channels use only minute quantities of lipid oil (less than 200 μ Ls) and sometimes also help

(24) Xu, J.; Sigworth, F. J.; Lavan, D. A. *Adv. Mater.* **2009**, *21*, 1–8.

(25) Stanley, C. E.; Elvira, K. S.; Niu, X. Z.; Gee, A. D.; Ces, O.; Edel, J. B.; deMello, A. J. *Chem. Commun.* **2010**, *46*, 1620–1622.

(26) Dixit, S. S.; Kim, H.; Vasilyev, A.; Eid, A.; Farris, S. G. *Langmuir* **2010**, *26*, 6193–6200.

(27) Heron, A. J.; Thompson, J. R.; Mason, A. E.; Wallace, M. I. *J. Am. Chem. Soc.* **2007**, *129*, 16042–16047.

(28) Heron, A. J.; Thompson, J. R.; Cronin, B.; Bayley, H.; Wallace, M. I. *J. Am. Chem. Soc.* **2009**, *131*, 1652–1653.

(29) Mugele, F.; Baret, J.-C. *J. Phys.: Condens. Matter* **2005**, *17*, R705–R774.

(30) Shama, R.; Andelman, D.; Berge, B.; Hayes, R. *Soft Matter* **2008**, *4*, 38–45.

(31) Babakov, A. V.; Ermishkin, L. N.; Liberman, E. A. *Lett. Nat.* **1966**, *210*, 953–955.

(32) Rosen, D.; Sutton, A. M. *Biochim. Biophys. Acta* **1968**, *163*, 226–233.

(33) White, S. H. *Biophys. J.* **1970**, *10*, 1127–1148.

(34) Wobschall, D. J. *Colloid Interface Sci.* **1972**, *40*, 417–423.

(35) White, S. H.; Thompson, T. E. *Biochim. Biophys. Acta* **1973**, *323*, 7–22.

(36) Requena, J.; Haydon, D. A. *J. Colloid Interface Sci.* **1975**, *51*, 315–327.

(37) Alvarez, O.; Latorre, R. *Biophys. J.* **1978**, *21*, 1–17.

(38) White, S. H.; Chang, W. *Biophys. J.* **1981**, *36*, 449–453.

in confining aqueous droplets from rolling over in the XY plane randomly. It is worth noting that the microchannels had *flat bottom surface* which served as substrate for DIB experiments. This provided *anchor-free* lipid monolayer coated droplets, as opposed to surfaces with dimples which distort the droplet shape.

D. Experimental Setup. Experiments were carried out on the stage of a Nikon Eclipse Ti-U inverted fluorescent microscope with a Nikon DS-Qi1Mc monochrome camera and NIS-Elements Basic Research software. The experimental setup consisted of a 0.5 μL microsyringe (Stoelting Co.) to dispense the lipid oil, an Agilent E3612A DC power supply, an HP4275A multifrequency LCR meter, 125 μm wide Ag/AgCl electrodes. A 5% wt/vol “agarose in PBS” hydrogel was coated on the tips of electrodes⁸ for making good electrical contact with droplets. For electrical current recording of DIB ion channels, a PicoAMP 300B BLM amplifier (Eastern Scientific LLC) was used along with an ADA 1210 DAQ analog-to-digital converter and TracerDAQ software. Current recording was performed inside a homemade Faraday cage, as shown in the experimental setup in Figure S1 in the Supporting Information.

E. Experimental Protocol. Typical procedures for performing DIB experiments are detailed here. Ag wire electrodes (10 cm long and 125 μm diameter) were chlorinated in 200 mM KCl at constant current for ~ 30 min using a chlorinator (Eastern Scientific, LLC). For current recordings, one end of each electrode is soldered to a 1 mm gold plated male pin and inserted in the head stage of an amplifier while the other end of electrode is dip coated slightly with “5 wt % agarose in PBS”. For experiments that involve external voltage sources other than the bilayer amplifier (such as LCR meter, signal generator etc.), the other end of the Ag/AgCl electrode is connected to the respective low noise cables coming from the equipment.

The agarose coated end of the Ag/AgCl electrode is attached to a micromanipulator. Lipid oil is sonicated for ~ 15 – 20 min before experiment. Microliters (typically $< 200 \mu\text{L}$ s) of lipid oil are dispensed into a clean, flat bottom plastic channel using a pipet. The droplets are then dispensed into the channel using a microsyringe. The microchannel with DIB and associated accessories are placed on the stage of microscope. Droplets bound to the agarose-coated electrode are moved by adjusting the micromanipulator. After allowing 20 min for coating with a lipid monolayer, the droplets are brought into contact to form the DIB. The initial DIB dimensions are determined by the size of the droplets and the slight force used in making the contact. After initial DIB formation, no mechanical force is applied. The microscope stage is surrounded by a fine copper mesh that serves as a Faraday cage (see Figure S1 in the Supporting Information). Simultaneous with electrical measurements, the DIB interface is recorded using either video or digital images through the microscope system. All data recordings are performed under dark room conditions. The currents, which experience random fluctuation with time, are recorded for ~ 30 s at each voltage level (20 mV increments). An example of minimum, average, and maximum current values as a function of applied voltage is shown in Figure S2a in the Supporting Information.

To confirm the presence of a lipid monolayer around each droplet, a simple experiment was conducted in oil without lipids. In the absence of lipids, when two aqueous droplets were brought into contact, fusion occurred instantaneously. In contrast, when lipids were present in the oil, fusion of aqueous droplets in contact did not occur. Fluorescein DHPE was used to confirm lipid monolayer formation. When excited at 488 nm, green fluorescein emission from the surface of the droplets is observed, indicating the presence of a lipid monolayer. Optical and fluorescent images of various aqueous droplets in dodecane lipid oil are shown in Figure 2. Stable DIBs have been formed using droplets with volumes ranging from picoliters to microliters. DIBs have been characterized by several methods: (a) electrically (capacitance and resistance); (b) optically (bright field and fluorescence imaging); (c) mechanically (use of slight force to modulate the DIB area);

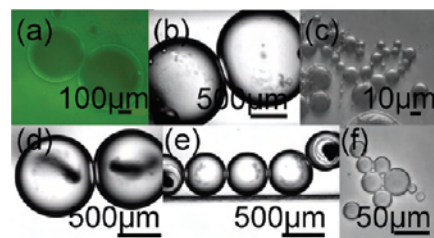


Figure 2. Microscopic images of some DIBs formed between: (a) ~ 100 nL DI water droplets in dodecane–DOPC–fluorescein DHPE; (b) $\sim 1 \mu\text{L}$ 1 \times PBS droplets in dodecane–DOPC–fluorescein DHPE; (c) picoliter DI water droplets in dodecane–DOPC–fluorescein DHPE; (d) 500 nL “150 mM KCl–10 mM HEPES” droplets in dodecane–DPhPC; (e) network of 100 nL “150 mM KCl–10 mM HEPES” droplets in dodecane–DPhPC; (f) nanoliter “150 mM NaCl” droplets in dodecane–DOPC–fluorescein DHPE.

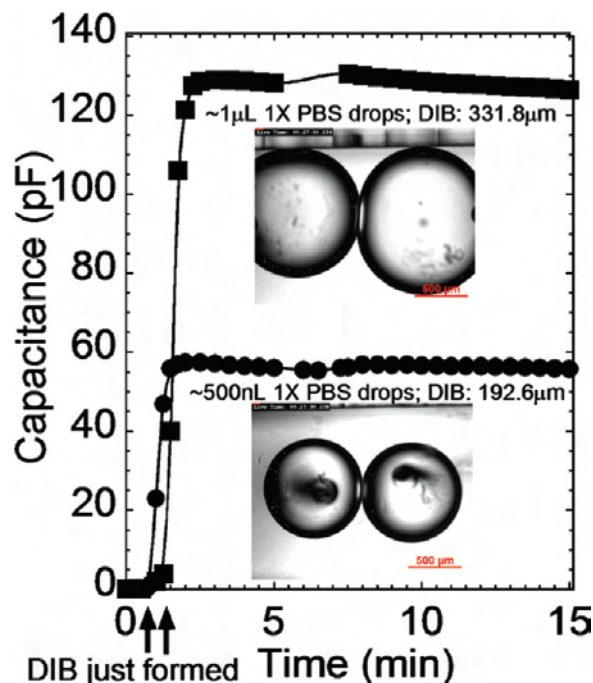


Figure 3. Droplet capacitance vs time at 113 mV peak-to-peak (40 mV rms) 10 kHz indicating point of DIB formation between 1 \times PBS (pH 7.4) droplets in dodecane–DOPC–fluorescein DHPE: (top) $\sim 1 \mu\text{L}$ droplets; (bottom) ~ 500 nL droplets.

(d) stability with time. Results from (c) and (d) are not included in this paper.

F. Electrowetting Fabrication. The EW structure was fabricated on a glass substrate coated with an indium tin oxide (ITO) layer (~ 150 nm) which served as a transparent electrode. The dielectric consisted of a thin layer of Al_2O_3 (~ 100 nm) deposited by atomic layer deposition (ALD). The final step is the spin coating of a thin film (~ 40 nm) of the fluoropolymer Fluoropel. After curing the Fluoropel layer, ohmic contact was made to the ITO electrode, and the sample was placed in a transparent rectangular plastic container filled with dodecane oil.

III. Results

A. Capacitance of DIB Lipid Membrane. The typical capacitance range¹ of artificial lipid bilayers is 0.5 to 1 $\mu\text{F}/\text{cm}^2$. The DIB capacitance was measured using the HP4275A LCR meter. Molten agarose hydrogel was coated on the tips of 125 μm wide Ag/AgCl electrodes, which were then attached to the

droplets. To measure the capacitance, a 113 mV peak-to-peak (equivalent to 40 mV rms) 10 kHz sine wave was used with the electrodes inserted into the droplets. The capacitance was monitored with time as the droplets are brought into contact to form the DIB. Figure 3 shows the capacitance versus time for the DIBs formed in DOPC dodecane oil. One DIB used ~ 500 nL of $1 \times$ PBS droplets, and the other DIB used $\sim 1 \mu\text{L}$ of $1 \times$ PBS droplets. When the droplets were brought into contact to form the DIB, the capacitance suddenly increased and then stabilized over time. The lateral extent of the DIBs was measured using the NIS Elements software. The droplets are not truly spherical on the substrate. When the droplets come in contact with the substrate, they assume flattened sphere geometry. The height of the DIB cannot be measured using the bottom up view in the microscope. Based on observations of many droplets, the DIB geometry was taken as approximately that of an ellipse whose minor diameter was equal to one-half of the major diameter (i.e., the measured DIB lateral length). For example, for the PBS droplets shown in Figure 3, at a time of 15 min, the DIB lateral lengths and capacitances, respectively, were measured to be $331.8 \mu\text{m}$ and 126.5 pF for a $1 \mu\text{L}$ PBS droplet DIB and $192.6 \mu\text{m}$ and 55.75 pF for a 500 nL PBS droplet DIB. Assuming the heights of DIBs as 165.9 and $96.3 \mu\text{m}$, the capacitances per unit area (specific capacitance) were calculated as 0.29 and $0.38 \mu\text{F}/\text{cm}^2$, respectively. These capacitances are in reasonable agreement with reported values,⁷ which fall typically in the $0.3\text{--}1 \mu\text{F}/\text{cm}^2$ range.

B. Effect of Voltage on DIBs. The effect of voltage on DIB properties was investigated as a function of several parameters: droplet volume, droplet composition (DI H₂O and various saline solutions), placement of electrodes, and DC vs AC bias. In all these cases, voltage controlled the dimensions of the DIB lipid membrane. DIB overlap increased with increasing voltage. This DIB dependence on voltage is reversible, but there is minor hysteresis in the process (see Figure S3 in the Supporting Information). DIB breakdown typically occurred above $200\text{--}300 \text{ mV}$ DC. In general, robust DIB dimension control under varying electric fields (below DIB breakdown range) was found for various droplet geometries and compositions.

The conductance of DIB without ion channels was in the $0.1\text{--}0.5 \text{ nS}$ range, which is comparable to the level typically reported in the literature. Nonlinear changes in DIB lateral dimensions and current as a function of voltage were observed. Since the current density was not constant with voltage (changing by $\sim 0.5 \mu\text{A}/\text{cm}^2$ from 0 to 100 mV), this indicates that the observed increase in conductance is not only due to the increase in DIB area. Other possible causes include (a) the inherent porosity arising from the zipping of loosely packed lipid monolayers on curved droplet surfaces near periphery of original DIB interface upon voltage increase; (b) increasing electroporation with voltage. Electroporation is likely to be a minor contribution, since the currents at higher voltages are stable with time and the process is reversible and repeatable.

The effect of DC voltage on DIB lateral length is illustrated in Figure 4. Figure 4a shows DC voltage induced changes in DIBs formed between two “ $150 \text{ mM KCl}\text{--}10 \text{ mM HEPES}$ ” (pH 7.4) droplets in DPhPC dodecane. Figure 4b shows microscopic images of the same DIBs at different DC voltages (-160 , 0 , and 160 mV). The error in precisely measuring the DIB lateral length is typically $\sim 1 \mu\text{m}$, and this applies to all DIB measurements. Increasing the DC voltage resulted in a nonlinear increase in the measured DIB lateral dimension. The estimated DIB area is plotted as a function of the square of voltage (V^2) in Figure 4c. The 500 nL case shows a linear relationship with V^2 over the entire range, while the 100 nL case showed a linear relationship up to

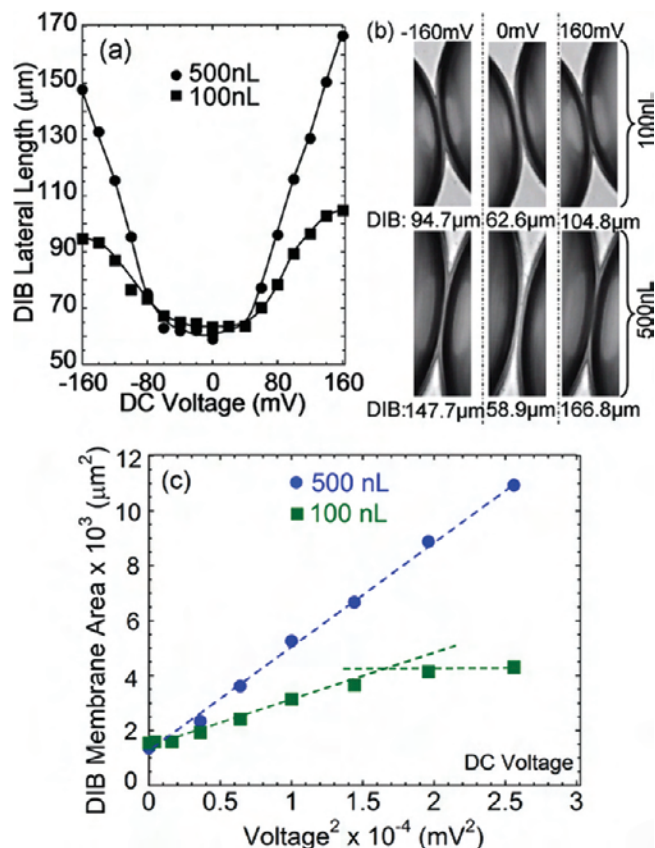


Figure 4. Effect of DC voltage on DIB lateral length for two sets of DIBs formed between “ $150 \text{ mM KCl}\text{--}10 \text{ mM HEPES}$ ” droplets in dodecane–DPhPC: (a) plot of DIB lateral length vs DC voltage for 100 nL and 500 nL droplet DIB; (b) microscopic images of two sets of DIBs at different DC voltages; (c) DIB area vs square of voltage.

120 mV followed by saturation. The saturation for smaller droplets indicates that droplet size has a major role in the observation of voltage effect on DIB dimensions. Other parameters that may be involved in saturation effects are the relative size of the electrode to the droplet volume and the relative size of the DIB length to the droplet diameter (related to the available surface-to-volume ratio). This effect is more pronounced for the smaller volume droplets, as the size of the wire electrode ($125 \mu\text{m}$ diameter) plus the swollen hydrogel coating on its tip is comparable to that of the droplet diameter. This square law dependence of DIB area on voltage has also been reported^{35,38} for conventional lipid bilayers. However, in the DIB case, the area changes are of the order of $100\text{--}500\%$ as compared to $1\text{--}20\%$ for the conventional case.

The effect of AC voltage on DIB properties was also investigated. Figure 5 shows the effect of 10 kHz sinusoidal AC voltage on the same volume and composition of droplets used for Figure 4. The capacitance and the DIB lateral length are shown in Figure 5a and b. As in the DC bias case, increasing the AC voltage resulted in increasing DIB dimensions and capacitance. The estimated DIB area and the associated specific membrane capacitance (C_m) for the 100 nL case are plotted as a function of V^2 in Figure 5c. Both the DIB area and C_m show an initial linear relationship with V^2 up to $141\text{--}170 \text{ mV}$ peak-to-peak ($50\text{--}60 \text{ mV}$ rms) followed by significant deviation from linearity. Similar dependence of lipid membrane C_m on V^2 has also been reported^{33,35} for conventional lipid bilayers. For these AC bias results, the C_m changes with voltage observed

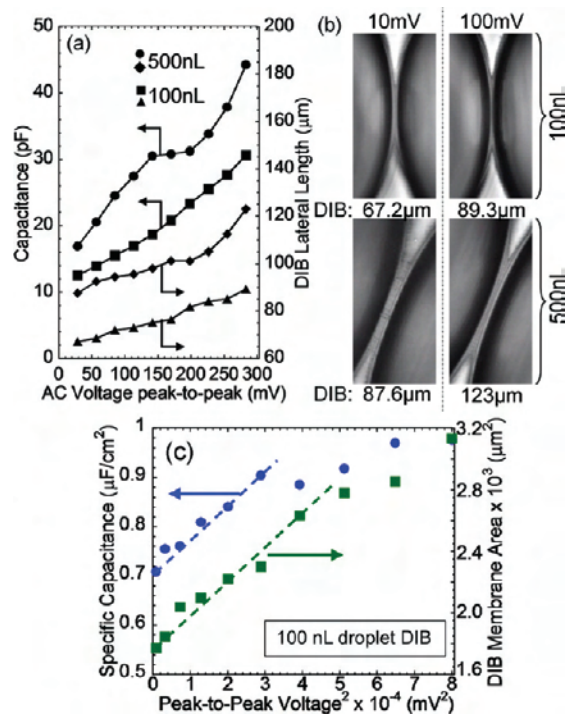


Figure 5. Effect of AC peak-to-peak voltage at 10 kHz on DIB lateral length for two sets of DIBs formed between “150 mM KCl–10 mM HEPES” droplets in dodecane–DPhPC: (a) plot of DIB lateral length vs AC voltage for 100 nL and 500 nL droplet DIB; (b) microscopic images of two sets of DIBs at different AC voltages; (c) DIB area and specific capacitance vs square of voltage.

for DIBs are slightly higher than those for conventional membranes.

C. Ion Channels in DIBs. As discussed above, inserting the electrodes in the droplets provides good control of DIB dimensions at DC or AC voltage levels of tens of millivolts. This is very important for ion channel and other transmembrane studies. Ion channel currents are typically measured at less than ± 100 mV to minimize current contributions from electroporation.³⁹ Controlling DIB dimensions significantly over the range of 10–100 mV indicates that it is possible to actively control the number of ion channels in the DIB by varying the applied voltage. This is discussed in the next section.

Alpha-Hemolysin (α HL) Currents across DIB. α HL is a pore forming transmembrane protein whose monomers assemble on lipid bilayers to form a heptameric β -helix structure that inserts itself into the lipid bilayer.^{40–42} Droplets containing about 25 ng/mL α HL mixed in “150 mM KCl–10 mM HEPES” (pH 7.18) were dispensed in dodecane–DPhPC oil. Agarose coated Ag/AgCl electrodes were inserted into the droplets of 500 nL. Ion channel currents were measured using the Picoamp 300B BLM amplifier.

Current versus time traces for α HL-containing droplets are shown in Figure 6 for -50 and -75 mV DC voltage. Ion channel activation steps are observed: ~ 24 pA change with respect to initial current for the 50 mV case; 33 and 50 pA change for the 75 mV case. These current steps are comparable to values reported¹²

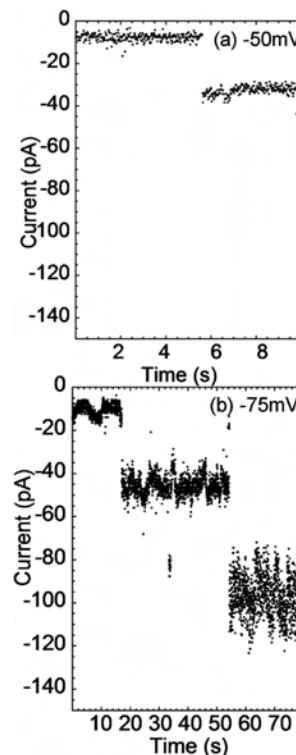


Figure 6. α HL ion channel currents in DIB formed in dodecane–DPhPC oil at (a) -50 and (b) -75 mV. Droplets: 500 nL, α HL (25 ng/mL); 150 mM KCl–10 mM HEPES (pH 7.18).

in the literature and show the well-known increased pore current with voltage. The noise level also increased with voltage, as can be seen in Figure 6b. As is the case with the other voltage induced-effects that we have observed, this could be due to a combination of the following factors: (a) increasing membrane area with voltage; (b) decreasing membrane resistance due to zipping of loosely packed lipid monolayers on curved surfaces of droplets near periphery of initial DIB. Similar increases in noise at higher voltage during alpha-hemolysin insertions have been reported.¹³

Effect of α HL Concentration on Ion Current. Bulk solution of α HL was prepared by mixing 5 μ g/mL α HL in DI water. An amount of 1 mL of buffer solution was prepared for each experiment by mixing 50, 100, and 200 μ L of “5 μ g/mL α HL DI water” solution with 950, 900, and 800 μ L of “150 mM KCl; 10 mM HEPES” buffer solution in order to obtain 0.25, 0.5, and 1 μ g/mL α HL buffer solutions, respectively. This approach of preparing desired solutions was purely due to convenience rather than rational. Due to this dilution process, the KCl concentration in new solutions was 142.5, 135, and 120 mM, respectively. Solutions were all at neutral pH. DIBs were formed in “dodecane–DPhPC” (5 mg/mL) using 500 nL droplets from each of these solutions. Ag/AgCl electrodes were inserted inside the DIB forming droplets, and DIB was formed prior to the voltage sweep. Voltage was increased from 0 to 100 mV in steps of 20 mV, in both positive and negative bias. Current and DIB lateral length were measured at each voltage level for different α HL concentrations. The average current for several α HL concentrations (from 0.25 to 1 μ g/mL) are plotted versus voltage in Figure 7a. A sample with no α HL (only 150 mM KCl–10 mM HEPES) was measured as a reference level for comparison. As expected, the current increased with α HL concentration at all voltage levels, with the effect being more pronounced at higher voltages. Average current densities and conductance/area are calculated. In Figure 7b, the upper half of the plot shows average current density while the lower half

(39) Chen, C.; Smye, S. W.; Robinson, M. P.; Evans, J. A. *Med. Biol. Eng. Comput.* **2006**, *44*, 5–14.

(40) Bhakdi, S.; Tranum-Jensen, J. *Microbiol. Rev.* **1991**, *55*, 733–751.

(41) Song, L.; Hobaugh, M. R.; Shustak, C.; Cheley, S.; Bayley, H.; Gouaux, J. E. *Science* **1996**, *274*, 1859–1866.

(42) Bayley, H.; Jayasinghe, L.; Wallace, M. *Nat. Struct. Mol. Biol.* **2005**, *12*, 385–386.

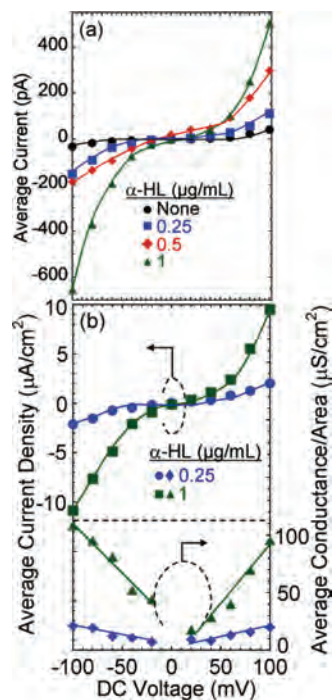


Figure 7. Effect of α HL concentration on DIB current with electrodes *inside* droplets: (a) average current vs voltage; (b) average current density and average conductance/area vs voltage. 500 nL KCl-HEPES droplets.

shows average conductance/area. For the highest α HL concentrations of 1 $\mu\text{g/mL}$, the average current density and DIB conductance/area, respectively, are approximately $10 \mu\text{A}/\text{cm}^2$ and $90\text{--}100 \mu\text{S}/\text{cm}^2$ at ± 100 mV bias. These values represent an order of magnitude increase over the “no α HL” case, even though the DIB dimensions are approximately the same at 100 mV for both cases.

In our anchor-free approach, the effect of increasing voltage on membrane current can be due to concomitant changes in DIB area (i.e., leakage current); conductance through additional pores in the increased DIB area; and increased individual pore conductance. We can rule out membrane leakage as a dominant effect, since the current measured in the absence of pores is relatively small (typically an average of ~ 15 pA at 60 mV, see Figure S2 in the Supporting Information) compared to the current when α HL is introduced (100s of pA, see Figure 7). However, it is difficult to unambiguously distinguish between the presence of additional pores and increasing pore conductance. Under our measurement conditions, we estimate that we typically have a very small number ($\sim 3\text{--}4$) of pores in the DIB at any one time. The observed increase in current with voltage in the $\sim 60\text{--}100$ mV is likely a combination of (1) the insertion of 1–2 additional pores ($60\text{--}100$ pA/pore \times 2 pores = $120\text{--}200$ pA) as the DIB area is increased; (2) increased conductance per pore (1 pA/mV \times 40 mV \times 4 pores = 160 pA). The total increase in current ($280\text{--}360$ pA) from the above estimate is lower than the observed change in current (~ 400 pA; see Figure 7a, 1 $\mu\text{g/mL}$ α HL case). Therefore, increased pore conductance cannot be the sole mechanism.

Overall, the results presented above show that as the voltage is increased the droplet interface increases, enabling more α HL proteins to be inserted in the increased lipid bilayer area. Additionally, the process is shown to be reversible and reproducible.

D. Comparison to Electrowetting Effect. As briefly mentioned in the Introduction, there are a priori similarities between the electric field control of DIB dimensions and the electric field

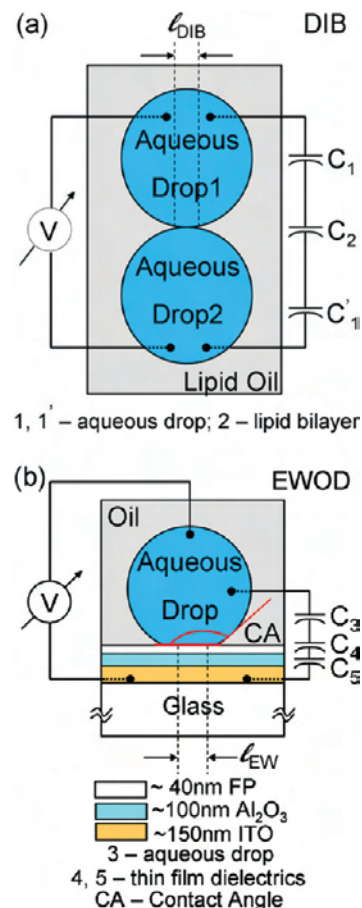


Figure 8. Schematic diagram of voltage control of droplet geometry: (a) droplet-on-droplet and (b) droplet-on-dielectric.

control of contact angle (CA) and contact length of droplets on hydrophobic surfaces. In this section, the DIB characteristics are compared to corresponding electrowetting characteristics of droplets. Investigations of the contact formed between twin aqueous droplets separated by a DIB and of the contact between an aqueous droplet and a solid surface are shown schematically in Figure 8. Both DC and AC voltage experiments were conducted. In DC voltage experiments, 500 nL DI water droplets were used and emphasis was given to CA measurements. In AC voltage experiments, 75 nL DI water droplets were used and emphasis was given to contact length measurements. To understand the role of various dielectrics in the path between electrodes, simple equivalent capacitive elements are shown for both DIB and EW cases in Figure 8b. C_3 , C_4 , and C_5 represent capacitances of the water droplet, hydrophobic fluoropolymer film, and inorganic dielectric layer, respectively.

The electrowetting structure shown in Figure 8b consists of a fluoropolymer thin film (which provides the hydrophobic surface) placed on top of a dielectric layer (which determines the capacitance of the structure) and an underlying metal electrode (ITO). This electrowetting-on-dielectric (EWOD) structure is stable with time, as it prevents electrochemical reactions at the electrode. The CA between the water droplet and the solid surface in the absence of voltage is determined by a balance of forces associated with the interface tension between the various materials involved (fluoropolymer surface, water and oil). Applying an increasing voltage results in an increased energy stored in the effective capacitance of the structure. This reduces the net surface energy of the system, decreases the CA, and increases the contact length

between the droplet and the solid surface, in other words wetting the surface. The EW CA is governed by the Young–Lippmann equation:^{29,30}

$$\gamma_{wo} \cos \theta_V = \gamma_{fo} - \gamma_{fw} + \frac{1}{2} CV^2 \quad (1)$$

where γ_{wo} , γ_{fo} , and γ_{fw} are the interfacial surface tensions between water droplet and oil, fluoropolymer surface and oil, and fluoropolymer and water, respectively. θ_V is the CA at applied voltage V , and C is the capacitance per unit area of the water/fluoropolymer region. Using θ_Y as Young's contact angle (i.e., at zero bias), the Young–Lippmann equation can be rewritten as

$$\cos \theta_V = \cos \theta_Y + W \quad (2)$$

where

$$W = \frac{1}{2} \frac{CV^2}{\gamma_{wo}} \quad (3)$$

W is the EW number which indicates the strength of the EW effect compared to the surface tension between water and oil.

DIBs were formed between touching water droplets in dodecane–DPhPC oil. In a DIB structure, the lipid bilayer itself plays the role of the thin film dielectrics in conventional EW structures. DIB contact angle change with voltage was calculated using the Young–Lippmann equation and the following material properties: lipid bilayer thickness of 5 nm, ϵ_r of 4.2 (from capacitance measurements), and γ_{wo} of 26 mN/m (ref 43). Experimental CAs for DIBs were measured as a function of voltage using droplet images and analyzed with the Image J program⁴⁴ customized for CA measurements.⁴⁵ For DIB experiments, two droplets of 500 nL DI water in dodecane oil were used. For the EW experiments, a single 500 nL DI water droplet was placed on the fluoropolymer (Fluoropel) surface surrounded by dodecane. A Ag/AgCl wire electrode was inserted in the droplet on the EW structure. With no voltage applied, the droplet remained nearly spherical with a CA at the junction of the droplet–Fluoropel interface and the droplet–dodecane interface of $\theta_Y = 172.5^\circ$. The combined thickness of thin film dielectrics was ~ 140 nm with an overall dielectric constant of ~ 4.2 . The interfacial surface tension between the aqueous droplet and the oil was taken as ~ 50 mN/m (ref 46).

Contact angles were measured as a function of DC voltage using the VCA Optima XE contact angle measurement system (AST Products, Inc.). CAs for DIB and EWOD are shown in Figure 9a and b, respectively. For both DIB and EWOD measurements, the bias electrodes were placed inside the droplets. For the DIB case, this limits the voltage range to a few hundred millivolts, beyond which the DIB breaks down and the droplets fuse. The CA at zero voltage is roughly the same for DIB and EWOD cases and, as expected, it decreases with increasing voltage in both cases. Theoretical (from eq 1) and experimental changes in DIB contact angle for the voltage range from 0 to -200 mV were 3.11° and 3.8° , respectively. The change in DIB lateral length was $38.36 \mu\text{m}$ for the same voltage range. This indicates that a 1° change in contact angle corresponds to a $10 \mu\text{m}$ change in DIB lateral length.

The changes in contact angle for both DIB and EWOD are plotted versus V^2 in Figure 9c and d, respectively. A reasonably good fit to a linear relationship is observed in both cases. This linear dependence of contact angle changes with V^2 is predicted by

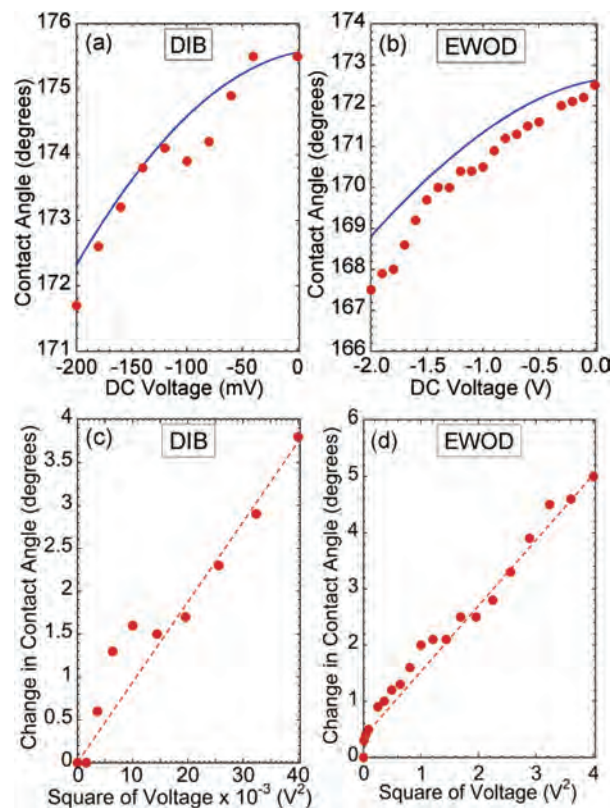


Figure 9. Contact angle vs DC voltage for 500 nL DI water droplets: (a) DIB and (b) EWOD. Change in contact angle vs square of voltage (c) DIB and (d) EWOD.

the modified Lippmann equation (eq 1) and has also been reported³⁶ for conventional lipid bilayers.

While the changes in CA in Figure 9a and b are roughly the same ($4\text{--}5^\circ$), the voltage range for the DIB data is $10\times$ smaller than the range used for the EW experiment. This highlights the much greater CA sensitivity to DC voltage of the DIB ($\sim 19^\circ/\text{V}$) compared to the EWOD ($\sim 2.5^\circ/\text{V}$). This is due to the fact that for these DIB measurements the electrodes are placed *inside* the droplets. In this situation, the significant difference in dielectric thickness between EWOD (140 nm) and DIB (5 nm) results in a much larger electric field across the DIB membrane than the electric field at the droplet–fluoropolymer EWOD interface. The experimental results (shown as points) are in reasonable agreement with theoretical calculations (shown as solid line) using above-mentioned parameters for the Young–Lippmann equation.

The effect of AC voltage on contact length was measured for both DIB and EWOD cases. Triangular waveforms were applied using the RG-3 signal generator (Eastern Scientific, LLC). For the DIB measurements, two DI water 75 nL droplets were dispensed in dodecane–DPhPC lipid oil and the electrodes were placed just outside the droplets in order to be able to apply a larger voltage without fusing them. For the EWOD measurements, a single 75 nL droplet in dodecane oil was used. The DIB contact length was measured as described above. For the EWOD measurements, the contact length was measured using bottom-up view in a Nikon (Eclipse Ti-U) inverted microscope. Due to this view through the microscope, contact angles could not be measured. Hence, we did not show contact angle data for EWOD structure in the AC bias case.

An example is shown in Figure 10 for a 6 V peak-to-peak 0.25 Hz waveform. It is important to note that both the DIB and the

(43) Reis, P.; Miller, R.; Leser, M.; Watzke, H.; Fainerman, V. B.; Holmberg, K. *Langmuir* **2008**, *24*, 5781–5786.

(44) Wayne, R. *Image J*; Research Services Branch (<http://rsbweb.nih.gov/ij/>), NIH: Bethesda, Maryland, 1997.

(45) Brugnara, M. <http://rsbweb.nih.gov/ij/plugins/contact-angle.html>, 2004.

(46) Goebel, A.; Lunkenheimer, K. *Langmuir* **1997**, *13*, 369–372.

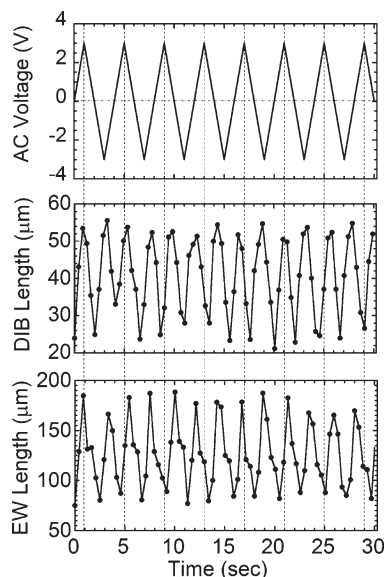


Figure 10. Contact length as a function of AC voltage waveform in DIB (electrodes *outside* droplets) and in EWOD; 75 nL DI water droplets at 0.25 Hz and 6 V (peak-to-peak).

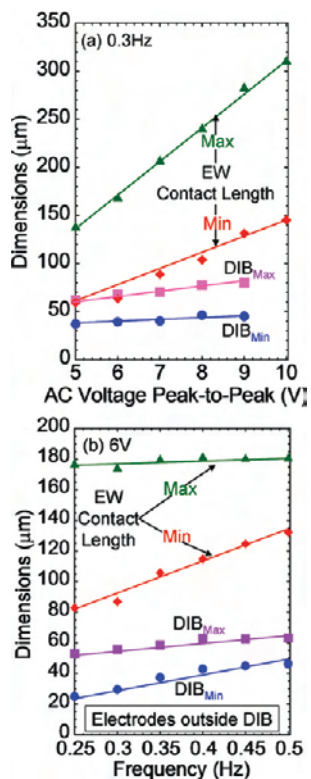


Figure 11. DIB lateral length (electrodes *outside* droplets) and EWOD contact length for 75 nL DI water droplets as a function of (a) voltage at fixed frequency (0.3 Hz) and (b) frequency at fixed voltage (6 V).

EWOD contact lengths vary at *twice* the frequency of the applied waveforms. In other words, the contact length varies with the amplitude of the waveform voltage and is not affected by the polarity of the waveform. The smallest values of the contact length (~ 20 to $30 \mu\text{m}$ for DIB and $\sim 80 \mu\text{m}$ for EWOD) occur at approximately the zero crossing of the waveform, while the largest values ($\sim 55 \mu\text{m}$ for DIB and $\sim 180 \mu\text{m}$ for EWOD) occur at the positive and negative peaks of the waveform.

Considering the response for any one-quarter cycle of the AC voltage, the normalized changes in contact lengths are computed for both EWOD and DIB. The observed normalized changes in DIB and EWOD contact lengths for 0–3 V at 0.25 Hz are 1.3 and 1.4, respectively. These normalized values for DIB and EW are in the same range. The implications of the similarity in response of the DIB and EWOD are further addressed in the Discussion section.

The effect of (low) frequency and voltage on EWOD and DIB contact length is seen in the data of Figure 11. In Figure 11a, the contact length maximum and minimum values are plotted versus peak-to-peak AC voltage at a fixed frequency of 0.3 Hz. Both EWOD and DIB values increase with voltage, with the EWOD increasing more rapidly. This is explained by the fact that, in this DIB case, with the electrodes *outside* the droplets, the voltage drop is only partly across the bilayer capacitance and partly across the oil layer capacitance and the monolayer capacitance. Therefore, the voltage effect is not as strong as in the EWOD case, where the electrode is placed inside the droplet and the voltage drop is mainly across the fluoropolymer/dielectric stack. In Figure 11b, the contact length maxima and minima are plotted versus frequency (0.25–0.5 Hz) at a fixed peak-to-peak voltage of 6 V. This frequency is low enough to allow observations (visually and by video recording) of DIB and EWOD changes as the AC voltage cycle goes through cycles. Once again, the EWOD and DIB share the same trends, albeit with differences in amplitude. In both cases, the maximum values are relatively unchanged with frequency while the minimum values increase significantly. Basically, this indicates that both DIB and EWOD droplets are able to dewet less and less (indicated by the minimum contact length at the zero crossing point) as the frequency increases. This is due to a combination of time constant limitation of droplet response and the frame rate limitation on the camera.

IV. Discussion

In this section, the main mechanisms of the effect of voltage on DIB properties are briefly examined. Relevant voltage-controlled mechanisms in electrofluidics include electrophoresis,⁴⁷ dielectrophoresis,⁴⁸ electrowetting,^{29,30} and the flexoelectric effect.⁴⁹ Generally, the electrophoretic and dielectrophoretic mechanisms result in one-directional force on charge particles and, hence, preferential motion dictated by the polarity of the electric field. Since the results presented here do not show a dependence on the electric field polarity, these mechanisms do not play a role. This is not unexpected, since only electrically neutral lipid molecules are used in the medium. The flexoelectric effect converts mechanical energy to electrical energy. In a membrane, the flexoelectric effect manifests itself through the generation of an electric potential across the membrane upon the application of mechanical force (hydrostatic pressure). Converse flexoelectric effect⁵⁰ causes a curvature change in the membrane when an electric field is applied. It should be noted that the converse flexoelectric effect is significant when the applied voltage across aperture-based bilayers is > 100 mV and if charged lipids are used. However, in the anchor-free DIB results reported here, neutral lipids are used and the applied voltages do not typically exceed 100 mV.

(47) Bier, M. *Electrophoresis: theory, methods, and applications*; Academic Press: New York, 1967; Vol. 2.

(48) Pohl, H. A. *Dielectrophoresis: the behavior of neutral matter in nonuniform electric fields*; Cambridge University Press: Cambridge, England, 1978.

(49) Petrov, A. G. *The Lyotropic State of Matter: Molecular Physics and Living Matter Physics*; Gordon and Breach Science: Amsterdam, The Netherlands, 1999.

(50) Todorov, A. T.; Petrov, A. G.; Fendler, J. H. *J. Phys. Chem.* **1994**, *98*, 3076–3079.

Furthermore, a key characteristic of the converse flexoelectric effect is that the frequency of curvature oscillation is the *same* as that of the applied voltage. In the results shown in Figure 10, the frequency of the DIB and EW contact length oscillations was *twice* that of the voltage waveform. This clearly indicates that the same mechanism is dominant for both DIB and EWOD oscillations, namely, the effect of potential on interfacial tension.

V. Summary and Conclusions

Anchor-free artificial DIB lipid membranes were formed at the interface of two aqueous droplets coated with lipids in dodecane lipid oil. The DIB approach is versatile, as it allows volume control of droplets, overlap control of droplets manually (mechanical) and electrically, formation of various types of bilayer networks, and separation and reformation. Most important is the voltage control of the DIB area. Significant increase in the DIB size with applied voltage was demonstrated for both DC and AC bias. *Simultaneous* optical and electrical observations on DIBs revealed nonlinear (mainly square law) changes in DIB lateral dimensions, currents, and capacitances with voltage. This voltage control process is reversible and reproducible. Results on DIB presented here augment earlier observations on conventional lipid bilayers and emphasize the

significance of voltage-induced effects on interfacial tension of lipid bilayers. Results presented on electrowetting on dielectric also exhibit a similar voltage effect on interfacial tension, causing changes in contact angle and contact length. This similarity is consistent with the fact that both effects are described by the Young–Lippmann equation.

Ion channel experiments were conducted with the transmembrane protein α HL as a function of voltage and concentration. Higher currents with increased voltage are estimated to be due to additional pore insertions into the extended DIB area rather than to increasing pore conductance. The EW-based control of DIB area enables active control of the number of ion channels available in the lipid bilayer membrane.

Acknowledgment. The authors appreciate useful technical discussions on EW with members of the Nanoelectronics Laboratory and Novel Devices Laboratory at the University of Cincinnati.

Supporting Information Available: Experimental setup for DIB; plots showing current vs voltage and current vs time across DIB; capacitance and DIB lateral length vs peak AC voltage plot and microscopic images. This material is available free of charge via the Internet at <http://pubs.acs.org>.

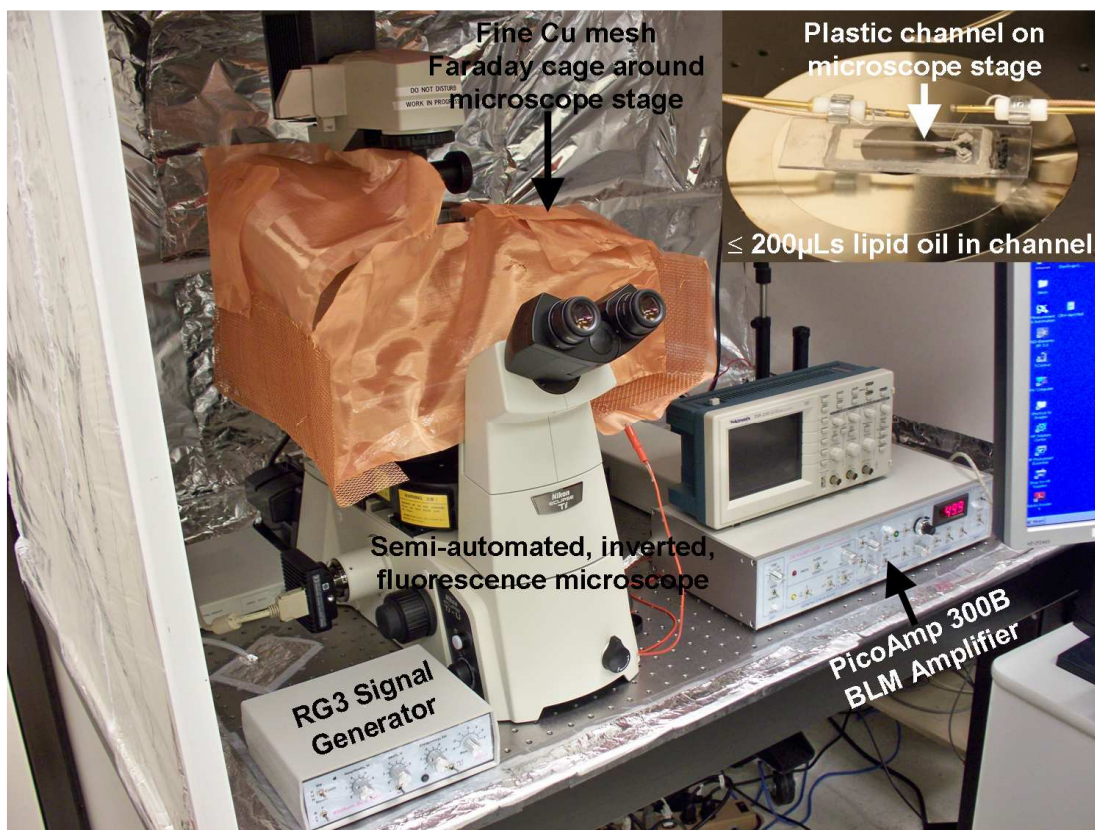


Figure S1. Experimental set up for DIB showing inverted microscope, home built faraday cage, BLM amplifier, signal generator, and oscilloscope. Inset shows microchannel and micromanipulator arms on microscope stage.

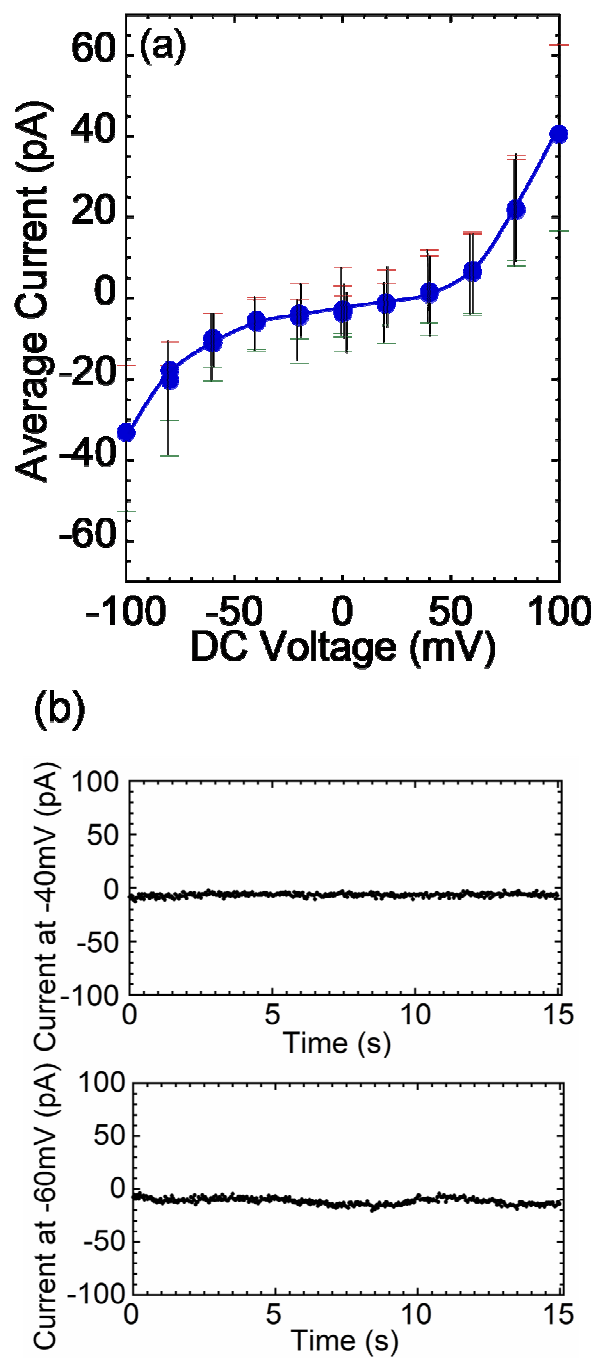


Figure S2. (a) Non-linear average Current-Voltage across DIB formed between two 500nL '150mM KCl-10mM HEPES' (pH 7.4) droplets in Dodecane-DPhPC (5mg/mL). Plot includes reversibility data (hysteresis insignificant). (b) Current traces with time across DIB without ion channels at -40 mV and -60 mV.

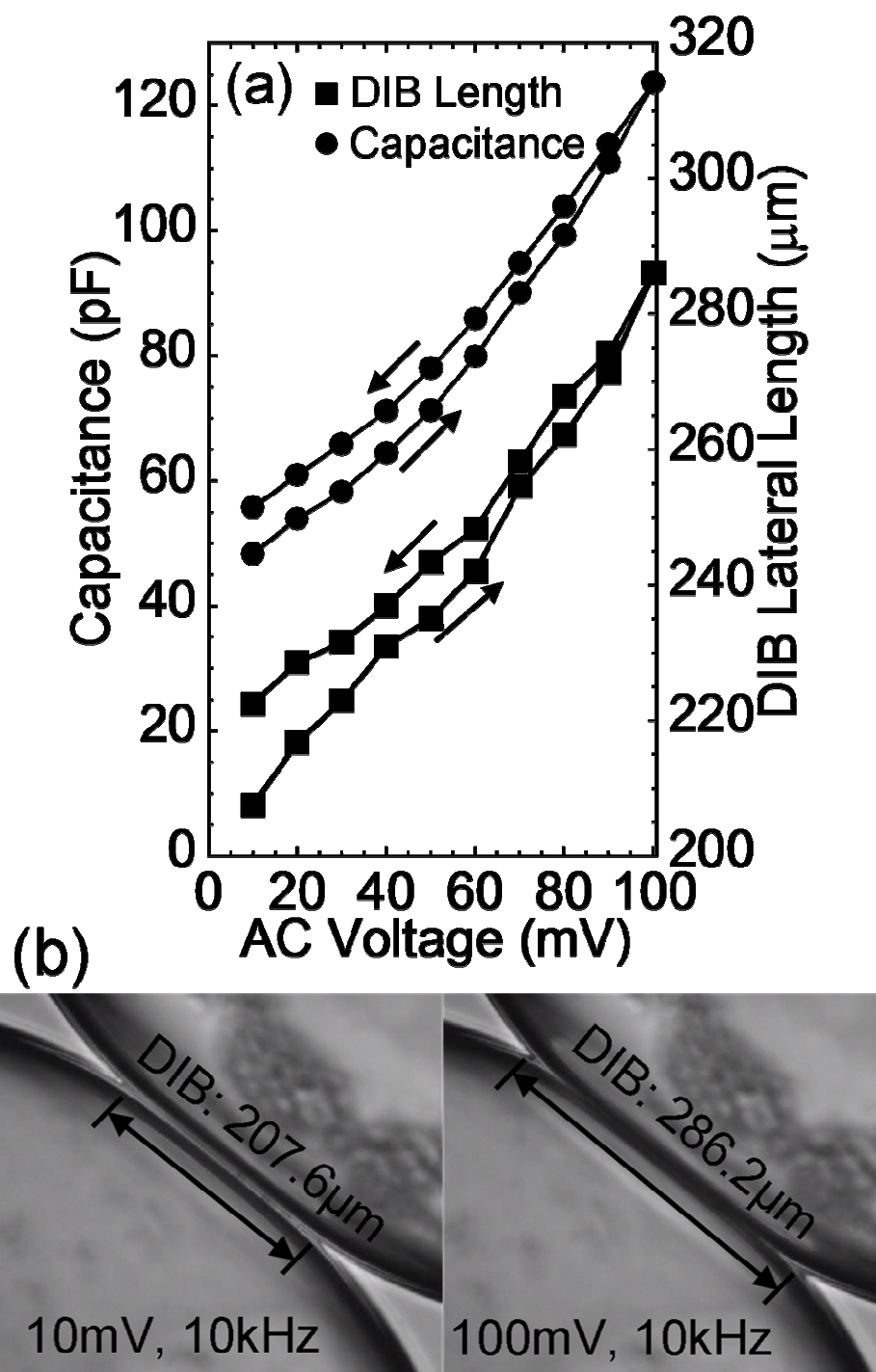


Figure S3. DIB, formed between two 500nL 1xPBS (pH7.4) droplets in dodecane-DPhPC (5mg/mL), showing minor hysteresis in AC voltage at 10kHz: (a) capacitance and DIB lateral length vs peak AC voltage; (b) microscopic images at different voltages.